



Synthesis, Crystal Structure, Spectroscopic and Antimicrobial Properties of Ruthenium Complexes of Vinyl Imidazole and 4-Ethylaminomethyl Pyridine Ligands

RINKI MONI KALITA¹, RAHUL SARMA BARUAH² and CHITRANI MEDHI^{1,*}

¹Department of Chemistry, Gauhati University, Guwahati-781014, India

²Department of Applied Sciences, Chemical Science, Gauhati University, Guwahati-781014, India

*Corresponding author: E-mail: chitranimedhi@gmail.com

Received: 13 December 2020;

Accepted: 9 February 2021;

Published online: 20 March 2021;

AJC-20295

Ruthenium complexes of vinylimidazole (VIMD) and 4-ethylaminomethyl pyridine (EMP) ligands were synthesized and characterized by XRD and spectroscopic methods. The binding of these Ru(III) complexes with calf thymus-DNA has been studied by UV-visible spectroscopic and electrochemical studies. A prominent increase in the intensity of fluorescence spectra of these complexes with CT-DNA was observed and a distinct UV-visible spectral shift in presence of CT-DNA is probably due to an interaction of these complexes with CT-DNA. The evidence of DNA binding has been found from the change in the intensity of fluorescence and UV visible spectra. Also, the electron transfer ability of these complexes is very important in order to rationalize their activity towards the biological system therefore, we have studied the electrochemical studies of these complexes by using cyclic voltammetry. From this study, it is possible to draw some ideas on electrochemical potentials of the complexes relevant to biological reduction possibly Ru(III)/Ru(II). Both complexes were also tested for antimicrobial activity against bacterial strain and responses well as antimicrobial agent.

Keywords: Ruthenium complexes, Vinylimidazole, 4-Ethylaminomethyl pyridine, DNA binding, CT-DNA, Cancer.

INTRODUCTION

Ruthenium(III) complexes containing biological active ligands have been known for their intriguing role in the area of anticancer drug design [1-5]. Considerable attention has been paid during the last decades to study the fused aromatic ligand complexes of ruthenium as DNA binding agent. The binding of ruthenium complexes originates from the Ru coordination as well as aromatic ligands interaction that the flat shape aromatic ligand are excellent molecule to recognize the complementary shapes of aromatic bases of DNA. In order to enhance the interaction of Ru complexes, it should be drawn considerable attention on the situation where the three interactions are predominant. They are (i) Ru coordination, (ii) the contribution of aromatic ring intercalation with DNA bases, and (iii) the configuration of ligands at the binding site. The aromatic ligands with extended π electrons to the aromatic ring such as imidazole derivatives have been used in several complexes. DNA binding of several ruthenium complexes have been reported where the flexibility of ligands at the binding site is also highlighted. Indeed Ru and Pt have similar metallic properties, the well-

known anticancer agent cisplatin has come up with the simple two NH_2 groups attached to platinum, but this complex is reported to be highly toxic. For this complex, the Pt coordination at N7 of guanine is the only binding after dissociation of Cl atom. On the other hand, Ru metal complexes are less toxic than cisplatin as reported in many literatures [5-10]. So, the geometry and electronic properties can be important to understand the more detail of the complexes for application to various areas. Due to presence of certain useful ligands in metal complexes anticancer or antitumor activity may be enhanced. Since the discovery of cisplatin, ruthenium complexes have been synthesized as potential candidate in the treatment of cancer and studied quite extensively due to their low toxicity and impressive biological activity [11-14]. Among the ruthenium complexes, NAMI-A and KP1019/KP1339 have entered clinical trials successfully [6-10,15,16]. It is due to the fact that ruthenium complexes offer a potential role as antitumor agents over platinum(II) complexes, with the properties of a novel mechanism of action, the prospect of non-cross-resistance, reduced toxicity and a different spectrum of activity [17,18].

Ruthenium complexes of vinyl imidazole (VIMD) and other pyridine complexes are found to be attractive agents and can interact with DNA efficiently. Ruthenium complexes can exist in different oxidation states (II and III) [5]. Several of ruthenium(II) and ruthenium(III) compounds with aromatic ligands are found as promising anticancer agents. The DNA binding ability of these complexes depends on the existence of stable oxidation state of the complex. It has been found that certain ruthenium complexes can act as pro-drug in Ru(III) oxidation states and on reduction to Ru(II) oxidation state in solid tumor masses where low oxygen content act as reducing environment [6,7]. There are several ruthenium(II/III) complexes containing 2,2'-bipyridine (bpy), 1,10-phenanthroline(phen) and *o*-phenyldiamine (*o*-phen) ligands. Most of these complexes can interact strongly with DNA and proteins [5,6]. The ligands, phen and bpy are semi-intercalators (wedging an opening between adjacent base pairs) or quasi-intercalation (indenture of one base pair) [7-9]. The bipyridine ligand has a tendency to align itself parallel with the base pairs with somewhat stacking interaction with DNA compared to phen ligand [10,15]. So ruthenium(II) complexes with bipyridine and *o*-phenyldiamine ligands may be good DNA binding agent that may be relevant to anticancer activity [5]. It has been reported that DNA binding affinity of ruthenium(II) bipyridyl complex can be enhanced by incorporating a carboxylic functionality. Furthermore, these compounds are also used for many purposes, like design and development of new drugs due to their potential for binding to DNA through multiple interactions.

Vinyl imidazole is one of the important ligands, which is also known to exhibit antibacterial, antifungal and other important biological activities. Some materials such as poly(*N*-imidazole) grafted chitosan, imidazole-imidazolium containing polymers, poly(3-hydroxyoctanoate) grafted vinyl imidazole *etc.* have been known for their antibacterial activities [19,20]. One of the advantage of using imidazole and its derivatives is that it can also achieve the stable configuration by undergoing various aromatic transformations in spite of their chemical and thermal stability of the ring. For this advantage of the aromatic ligands, such as vinyl imidazole and the heterocyclic ligands are strongly desired for improved and cost effective biological applications [21].

As we know that the heterocyclic compounds are often used in drug discovery because of their affinity towards biological system. Pyridine is six-membered heterocyclic compounds and its structural similarity in many naturally occurring bioactive compounds is remarkable. Pyridine derivatives display various biological properties antiviral, antitumour, analgesic, local anaesthetic, antimicrobial, fungicidal, herbicidal, insecticidal, antihistaminic, anti-inflammatory, anticancer, *etc.* [22-31]. So, we have synthesized Ru complexes with biologically active ligands, *N*-vinyl imidazole (VIMD) and 4-ethyl-aminomethyl pyridine (EMP). The complexes can be active anticancer compound, but sometimes low solubility in water is another disadvantage. In fact, the solubility may be enhanced by using DMSO molecules as ligand in ruthenium complexes. Hence, dimethyl sulfoxide (DMSO) complexes of both Ru(II) and Ru(III) are as good as cisplatin in terms of anticancer activity

[24-31]. Here, the present studies have been focused on the synthesis, characterization and DNA binding of Ru(III) complexes containing aromatic ligands and DMSO molecule.

EXPERIMENTAL

The solvents, dimethyl sulfoxide (DMSO) and ethanol were used as received. The compounds, 4-ethyl amino methyl pyridine and vinyl imidazole were also used in the synthesis without purification. Analytical grade RuCl₃·3H₂O, calf thymus DNA (CT-DNA) and Tris-buffer have been purchased from Sigma-Aldrich Chemical company. The CT-DNA was dissolved in 5 mM tris buffered saline (pH 7.4, TBS) and dialyzed overnight against the same buffer so that A₂₆₀/A₂₈₀ of the dialyzed solution can remain > 1.8.

Characterization: The IR spectra of the complex were recorded as KBr pellets on a Shimadzu IR Affinity-1 Perkin-Elmer FT-IR spectrophotometer. The UV-visible spectra were measured in DMSO solvent in a Shimadzu UV-2401 PC spectrophotometer.

Synthesis of ruthenium vinyl imidazole DMSO complex (Ru-VIMD): RuCl₃·3H₂O (0.1 g) was refluxed with 3 mL ethanol and 3 mL of 1N HCl for 1 h. The solution was cooled at room temperature before adding the ligand. Vinyl imidazole dissolved in 1 mL ethanol (1:1) and 1 mL of 5M HCl and added to the above solution. The mixture was stirred for 0.5 h and again 0.5 mL DMSO was added. The solution was further stirred for 0.5 h and refluxed at 50 °C for 1 h. After cooling the solution at room temperature, obtained red crystals were recrystallized from acetonitrile and methanol solution. IR (ν_{max}, cm⁻¹): 2956 (C-H methyl), 1556 (C=N arom.), 1424 (C = C), 1224 (C-N), 1103 (S=O for S bonded DMSO), 576 (Ru-Cl), 516 (Ru-N) and 833 (C-S, DMSO), 756 (C-H bending ring), 482 (Ru-O), 460 (Ru-S).

Synthesis of ruthenium 4-ethyl amino methyl pyridine DMSO complex (Ru-EMP): RuCl₃·3H₂O (0.1 g) was refluxed with 10 mL ethanol and 1 mL of 5N HCl for 1 h. After refluxing the solution was cooled at room temperature. Ligand 4-ethyl aminomethyl pyridine ligand dissolved in 1 mL ethanol (1:1) and 2 mL of 5M HCl by slow heating. The solution was further refluxed for 1 h and then 0.5 mL DMSO was added after cooling the solution. The solution was further refluxed at 50 °C for 1 h. After cooling at room temperature, obtained orange crystals was recrystallized from acetonitrile and methanol. IR (ν_{max}, cm⁻¹): 3417 (-NH proton), 2985 (C-H methyl), 1562 (C=N arom.), 1463 (C = C), 1298 (C-N), 1078 (S=O for S bonded DMSO), 820 (C-S, DMSO), 634 (Ru-Cl), 507 (Ru-N) and 472 (Ru-O).

Crystallography of complex: Fine crystals were selected and mounted on glass capillary and data were collected at room temperature. Single crystal X-Ray diffraction data were recorded at 100 K with Bruker smart ARES2 diffractometer with graphite-monochromatized Mo-Kα radiation by φ-ω scans. The molecular graphic structure was analyzed by ORTEP plot program. Crystal dimensions were determined from the setting angles. The structures were solved by the Patterson method. SHELXTL routine analysis was used for empirical absorption correction.

Antimicrobial activity: The *in vitro* antibacterial activities of the ligands and metal complexes were investigated using Gram-positive bacteria, Gram-negative bacteria and yeast by applying the disc diffusion method. Antimicrobial activity of Ru(VIMD) and Ru(EMP) complexes were tested against four bacterial strains such as *Staphylococcus aureus*, *Klebsiella pneumoniae*, *Acinetobacter baumannii*, *Pseudomonas aeruginosa* and one fungal/yeast strain *Candida albicans* by agar well diffusion method. A lawn of microorganisms was prepared by pipetting and evenly spreading inoculums onto agar set in petri dishes, using nutrient agar for the bacteria. The plates were incubated for 24 h at 37 °C. The stock solutions were prepared in dimethyl sulfoxide. The presence of clear inhibition zones around the discs indicates the antimicrobial activity of complex. Same concentrations of both the complexes were used in this study.

RESULTS AND DISCUSSION

IR studies: The coordination of Ru with aromatic ligand in Ru-VIMD complex at 516 cm⁻¹ (Ru-N) was shown and the corresponding values for Ru (EMP) was observed at 507 cm⁻¹ (Ru-N). The shift in Ru-ligand bonding is also indicative of the strength of Ru-ligand coordination bond. EMP ligand is better electron density donor than VIMD, which thereby resulted strengthening the coordination bond.

¹H NMR spectra: The ¹H NMR spectra have been recorded on a Bruker DPX 300MHz NMR spectrometer using TMS as the internal standard. ¹H NMR signals for Ru-VIMD complex were observed at 7.83 ppm and 5.89 ppm H (imidazole) at 5.38 ppm (for =CH₂ vinyl) and 1.76 ppm for H (DMSO). ¹H NMR signals for Ru-EMP complex were observed at 6.63 ppm and 6.61 ppm for H (benzene ring) at 2.07 ppm (for -COCH₃) and 1.54 ppm (for H DMSO).

UV-visible spectra: The UV-visible absorption spectra of ruthenium complexes in DMSO solution showed two characteristic peaks near visible region. The λ_{max} value of Ru-VIMD and Ru-EMP complexes were recorded where intra ligand π-π* transition for these complexes were observed at 296 nm (Ru-VIMD) and 301 nm (Ru-EMP). LMCT transition for Ru-VIMD and Ru-EMP complexes were observed at 378 nm and 410 nm, respectively.

The electronic spectra observed two absorption bands, which are attributed to π-π* and n-π* transitions. The electronic spectra of the complexes at bands are due to the coordination of Ru with ligand. The higher energy absorption bands are assigned to intraligand π → π* transitions and lower energy absorption band were assigned to metal dπ → ligand pπ* MLCT transition. Both the complexes show a typical MLCT band in the range 400 nm to 500 nm. Inter-ligand transition band was observed in the range 250 nm to 300 nm.

UV-visible absorption titration: The measurement of UV absorption of compounds was conducted in the Tris HCl buffer (pH 7.4). The CT-DNA stock solution was added to a fixed concentration of complex and spectra were recorded for further increments of CT-DNA concentrations. The solutions were allowed to incubate for 30 min before the absorption spectra were recorded. After adding CT-DNA at different concentra-

tions shifting of spectra in the visible region at λ_{max} was observed. With the increase of the CT-DNA concentrations, the absorbance of the complex spectra decreases. These spectral characteristics suggest the possible interaction between the complex and CT-DNA.

Interaction of the complexes with CT-DNA was monitored by UV-visible absorption spectra. The experiment was performed by maintaining a constant concentration of the complex while varying the concentration of CT-DNA, from 0 to 2.37 × 10⁻⁵ M. The binding strength was estimated from the intrinsic binding constant, from the ratio of slope and intercept of the graph from the following equation:

$$\frac{[\text{DNA}]}{(\epsilon_a - \epsilon_f)} = \frac{[\text{DNA}]}{(\epsilon_b - \epsilon_f)} + \frac{1}{K(\epsilon_b - \epsilon_f)}$$

where ε_a, ε_f and ε_b are the extinction coefficient of, observed solution, free complex and the ruthenium complex, when it fully bound to CT-DNA, respectively. The binding constants for Ru-VIMD and Ru-EMP complexes are found to be 0.3181 × 10⁵ and 0.936 × 10⁵ M⁻¹ respectively. Fig. 1a-b represents the spectra of these complexes and with increasing concentrations of CT-DNA. On increasing the concentrations of CT-DNA, absorbance of both these complexes found to be decreases. Ru-VIMD complex was found to exhibit hypochromism at 378 nm (19.12%) and for Ru-EMP complex at 410 nm (32.10%).

Fluorescence emission studies: Emission and excitation spectra in buffer solution were recorded on a Hitachi EPA-2A fluorescence spectrophotometer, which contains a 150-W xenon lamp for excitation, a grating monochromator (600 grooves/mm, blazed at 300 nm) for exciting light and a grating monochromator (600 grooves/mm, blazed at 500 nm) for luminescence spectroscopy. The luminescence from the sample solution in a rectangular cell of 1 cm path length was detected by a Hamamatsu TV photomultiplier R-136 placed at right angles to the exciting beam. For most ruthenium complexes, presence of one or two chloride ion has been indicated for binding with DNA or proteins after dissociation of Cl atoms. Fluorescence emission study was performed by keeping the concentration of metal complex constant and followed by adding different concentrations of CT-DNA. On addition of several concentrations of CT-DNA, the emission intensities of this complex increases and implies the possible interaction of complex with CT-DNA. Emission intensity of complexes Ru-VIMD and Ru-EMP at exciting wavelength 280 nm are obtained and these are found to depend on DNA concentrations. Fig. 2a-b shows the emission spectra of Ru-VIMD and Ru-EMP complexes with different concentrations of CT-DNA. The binding of Ru complexes with CT-DNA were observed by monitoring the change in intensities of fluorescence spectra of these complexes but the emission wavelength was not changed. Concentrations of these metal complexes are kept constant throughout the experiment and fluorescence spectra were recorded after adding various concentrations of CT-DNA. It has been observed that emission intensity of complex Ru-VIMD shows 33.61% increase in presence of 2.37 × 10⁻⁵ M CT-DNA and for Ru-EMP in presence of 2.37 × 10⁻⁵ M CT-DNA, 83.21% increase in emission intensity is observed at 350 nm wavelength. As, it can be observed

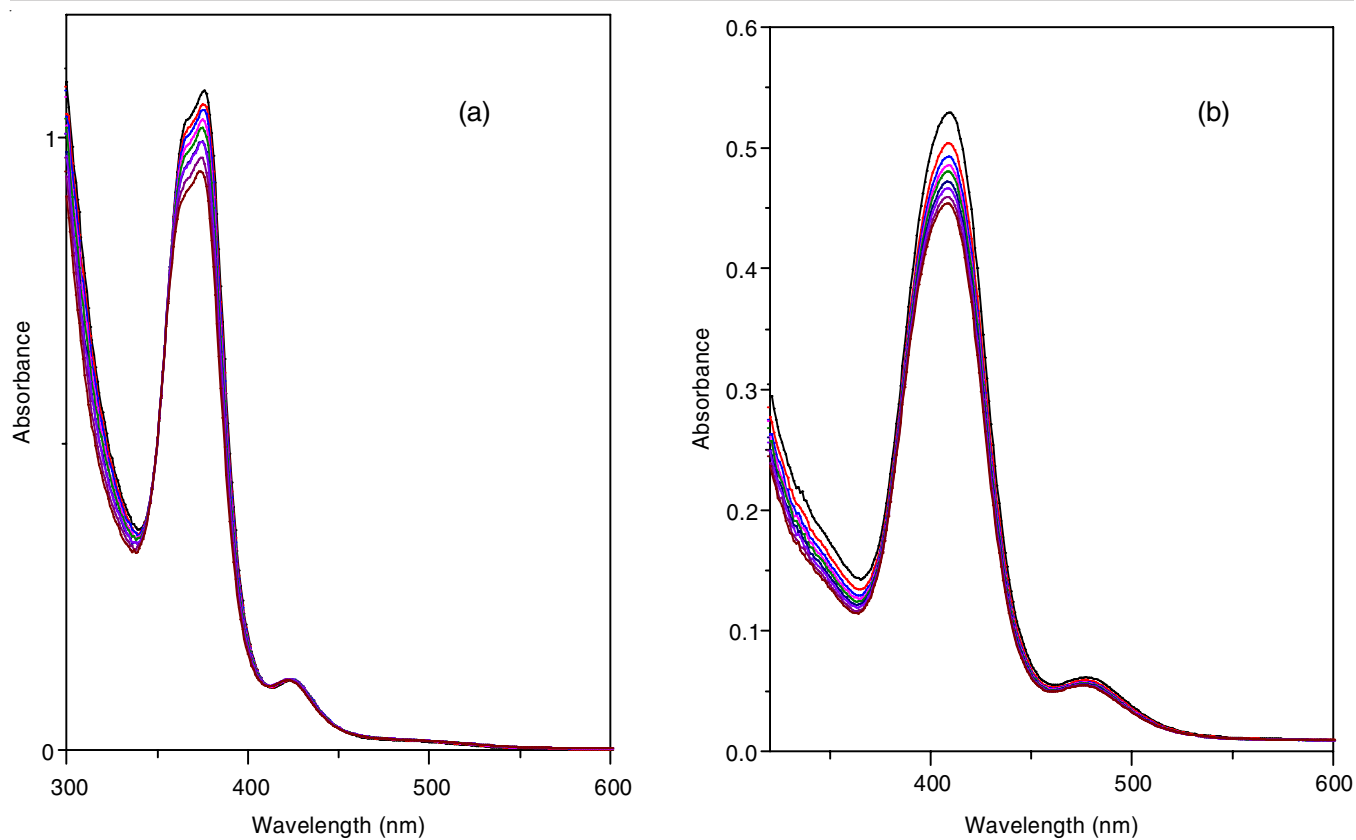


Fig. 1. UV-visible spectra of (a) Ru-VIMD and (b) Ru-EMP complex in Tris-buffer (pH = 7.4) with increasing concentrations of CT-DNA (from 0 to 2.37×10^{-5} M DNA)

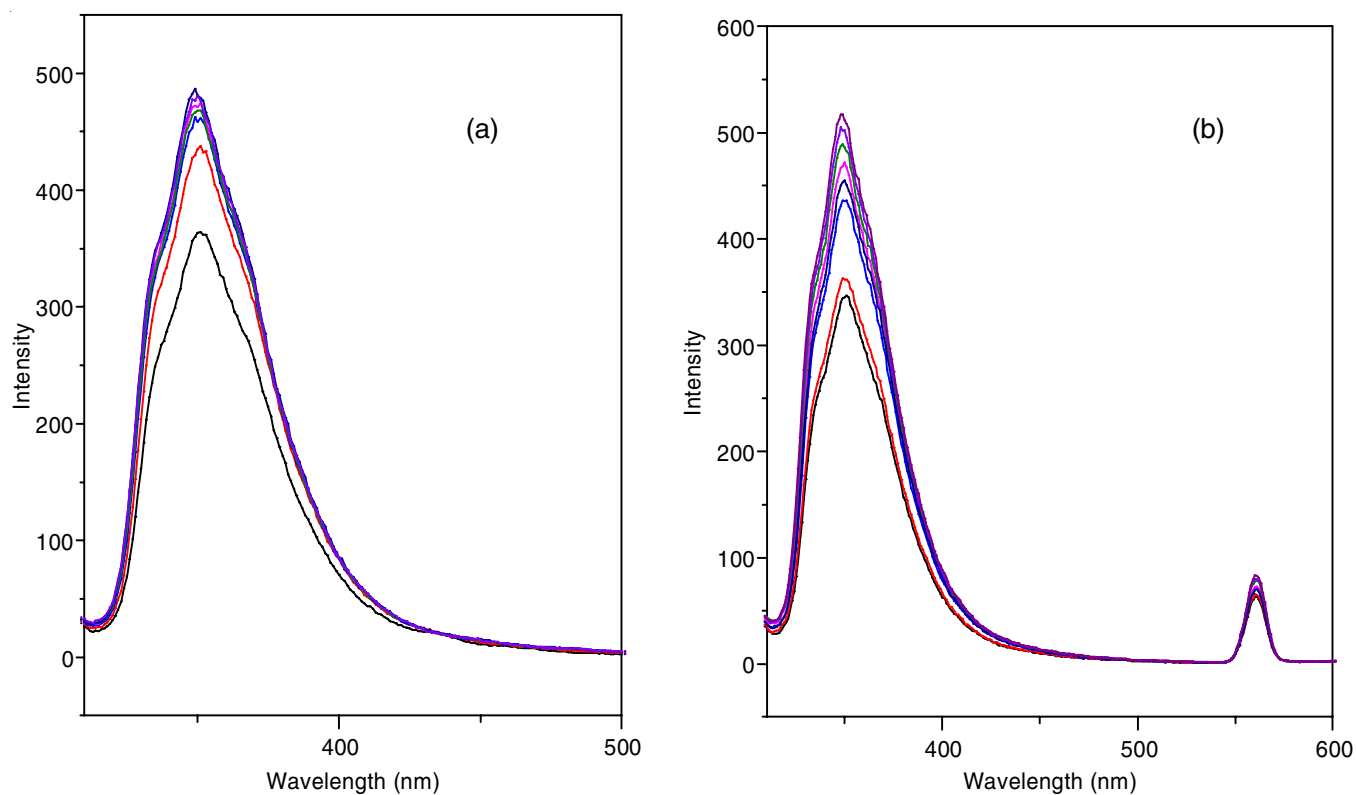


Fig. 2. Fluorescence spectra of (a) Ru-VIMD (b) Ru-EMP complex (exciting wavelength = 280 nm) with different concentrations of CT-DNA (from 0 to 2.37×10^{-5} M DNA)

that after adding CT-DNA, the emission intensities of this complex substantially increased and it implies the binding of this complex with DNA. In general, the hydrophobic environment inside the CT-DNA restricts the mobility of the complex from entry within DNA for binding, hence the observation clearly indicates the coordination of Ru complexes with certain site of DNA.

Cyclic voltammetry studies: In this work, synthesized Ru complexes were used for further electrochemical studies. The aim of this electrochemical study in presence of CT-DNA is to examine the change of redox potential due to DNA binding for further applications as anticancer agent or DNA cleaving agent. The voltammogram shows distinct oxidation and reduction peaks of a reversible electron transfer reactions. Cyclic voltammetric study of Ru-VIMD was carried out in DMSO solution containing TBAP as supporting electrolyte using Ag/Ag⁺ as reference electrode and a platinum electrode was used as working electrode. The inert environment was maintained by passing N₂ gas through the solution to remove oxygen. It was observed a positive shift of potential for Ru-EMP complex cathodic peak (E_c) occurs at 0.593 V and anodic peak (E_a) of Ru-EMP complex was found to be 0.678 V. After adding 20 μ L of 0.5 mM CT-DNA E_c occurred at 0.602V and E_a of Ru-

EMP complex was found to be at 0.683 V. Again for Ru-VIMD complex, cathodic potential shifts from 0.231 to 0.241 V and anodic potential 0.342 to 0.356 V after adding 20 μ L of 0.5 mM CT-DNA (Figs. 3 and 4). After adding 20 μ L of 0.5 mM CT-DNA, the current diminishes 12.28% for Ru-VIMD and 32.25% for Ru-EMP complex, respectively. The results indicate the possibility of binding of this complex with CT-DNA. Cyclic voltammograms of Ru-VIMD and Ru-EMP complexes at different scan rate (100-400 mV) are shown in Figs. 3 and 4, respectively. Plot of current vs. square root of scan rate are also shown in Figs. 3b and 4b. The electrochemical characteristics of the complex such anodic oxidation cathodic reduction of the redox potential clearly indicated the shifting towards the anodic after mixing with CT-DNA. It might be due to difference in electronic effect after binding with CT-DNA. However, the nature of binding can't be established from this experiment. It is therefore assumed that the complex might act as anticancer agent. Another point of view to be addressed about DNA binding is probably obtained from the understanding of redox reactions. Indeed the behaviours of oxidation and reduction potentials of these complexes vary to some extent and the corresponding plot with CT-DNA. Also the potential shifts resulting from the binding of complexes with CT-DNA could be due to change

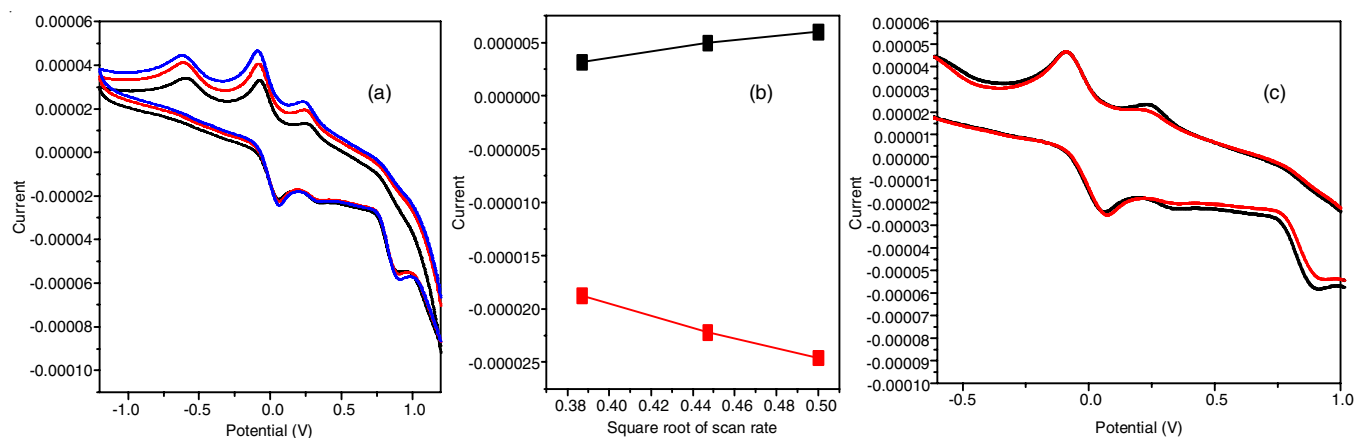


Fig. 3. Cyclic voltammogram of Ru-VIMD (a) at different scan rate, (b) plot of current vs. square root of scan rate for redox process (c) voltammogram of Ru-VIMD complex without DNA and 20 μ L of 0.5 mM CT-DNA

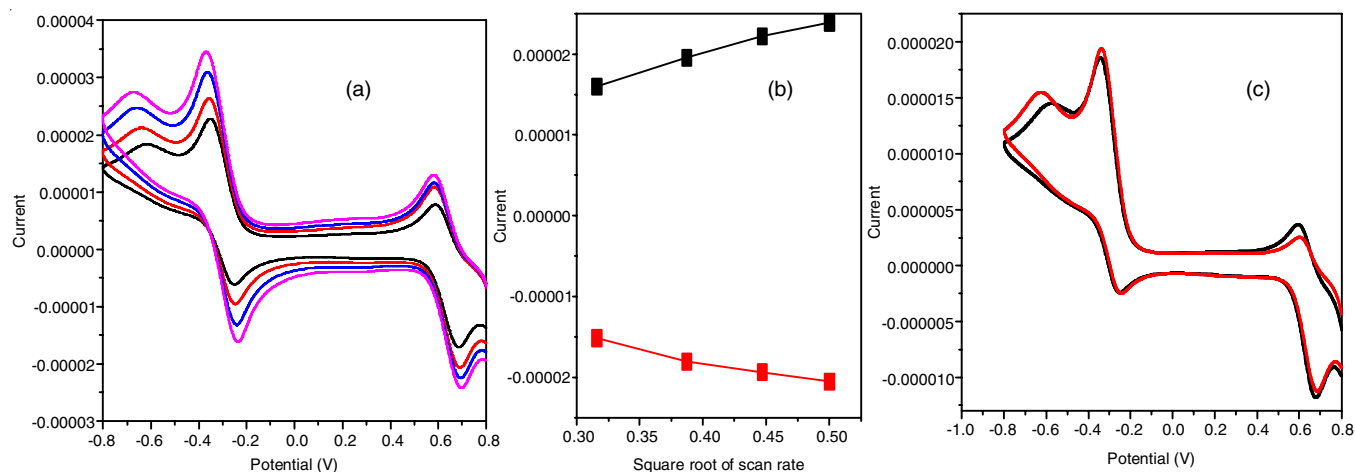


Fig. 4. Cyclic voltammogram of Ru-EMP (a) at different scan rate, (b) plot of current vs. square root of scan rate for redox process (c) voltammogram of Ru-EMP complex without DNA and with 20 μ L of 0.5 mM CT-DNA

of Ru(II) to Ru(III) or *vice-versa*. These results apparently indicate that Ru(II) or Ru(III) coordination with DNA is apparent since the potential shifts are found to be towards higher potentials, which may be interpreted due to CT-DNA binding with these complexes.

The presence of substituents can induces potential values, which is observed for these two different substituents *i.e.* VIMD and EMP, which contributes to the extent of potential shift as well as CT-DNA binding ability. The roles of electronic effect and the coordination ability of ligand with Ru can be highlighted in this aspect. Also more stable complex can produce less shift whereas more shift is expected for less stable complex. This trend is the same in regards of CT-DNA binding ability of these complexes. The chemical reaction involving this reaction is the electrochemical reduction capability of Ru(III) after binding with CT-DNA. However, ligand effect was ignored towards CT-DNA on the electrochemical shift due to Ru coordination. So, Ru(III) complex of VIMD shows better reduction reaction towards DNA. The nature of the voltamograms of the two complexes are almost similar. The shift in redox potential may be due to the involvement in Ru center in CT-DNA binding. In the sense, the reactivity or coordination ability of Ru towards donor sites of DNA might be related to difference in electrochemical shift.

Antimicrobial activity: The synthesized Ru complexes were screened *in vitro* for their antibacterial activities. The Ru-EMP complex shows low to moderate zone of inhibition against the studied bacterial strains. Ru-VIMD complex had again displayed moderate zone of inhibition against all the tested bacterial strain. From Fig. 5, it is evident that Ru-EMP complex show better antimicrobial property than Ru-VIMD complex. An increase in the bacterial activity is due to the effect of metal ion on the normal state of the cell progress other structural components may also be involved by inhibiting enzyme activity due to deactivation of metal coordination. The π -electrons may also involved by delocalization and thereby increases lipophilicity of the complexes. It forms the complex permeation through lipid bilayer of the cell membrane of bacteria.

Crystallographic studies: The crystallographic data collected for both Ru-VIMD and Ru-EMP complex are given in Table-1. The ortep diagrams of Ru-VIMD and Ru-EMP complexes are shown in Figs. 6 and 7. In the asymmetric structure

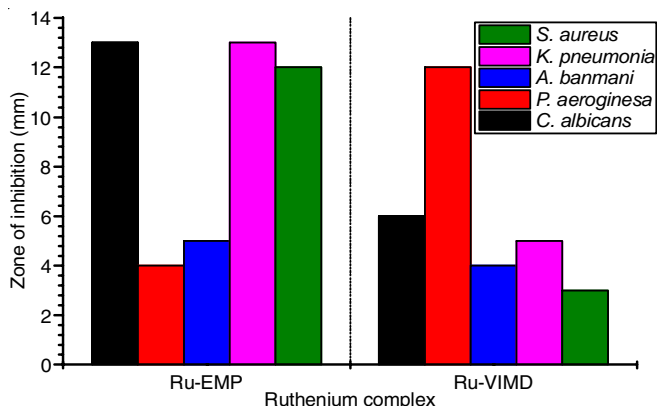


Fig. 5. Bar representation of zone of inhibition of Ru-VIMD and Ru-EMP complexes

TABLE-1
SUMMARY OF THE CRYSTALLOGRAPHIC
DATA COLLECTIONS FOR COMPLEXES

Parameters	Ru-EMP complex	Ru-VIMD complex
Crystal system	Triclinic	Orthorhombic
Wavelength	0.71073 Å	0.71073 Å
Space group	P 1	P bam
Empirical formula	C ₇₉ H ₁₇ N ₁₆ O ₁₀ S ₈ Cl ₃₂ Ru ₈	C ₁₁ HN ₄ OSCl ₄ Ru
Formula weight	3549.53	479.08
Z	1	4
Unit cell dimensions	a = 7.7110(5); b = 14.7774(11); c = 32.027(2) α = 88.153(4)°; β = 83.225(4)°; γ = 74.888(4)°	a = 13.5309(16); b = 20.971(3); c = 7.0987(8) α = 90°; β = 90°; γ = 90°
T (K)	296	296
Volume	3498.6(4) Å ³	2014.3(4) Å ³
Density	1.685 g cm ⁻³	1.580 g cm ⁻³
Absorption coefficient	1.619 mm ⁻¹	1.414 mm ⁻¹
T _{max} , T _{min}	29.431, 2.357	30.230, 1.325
R(reflections)	0.0778(20045)	0.1115(1627)
wR2	0.1982	0.3438
F(000)	1707.0	920.0
Index ranges	-10 ≤ h ≤ 10 -20 ≤ k ≤ 20 -44 ≤ l ≤ 44	-19 ≤ h ≤ 19 -29 ≤ k ≤ 29 -10 ≤ l ≤ 10
Reflections collected	49447	10348
No of parameters	1381	122
Goodness-of-fit on F ²	1.153	1.096

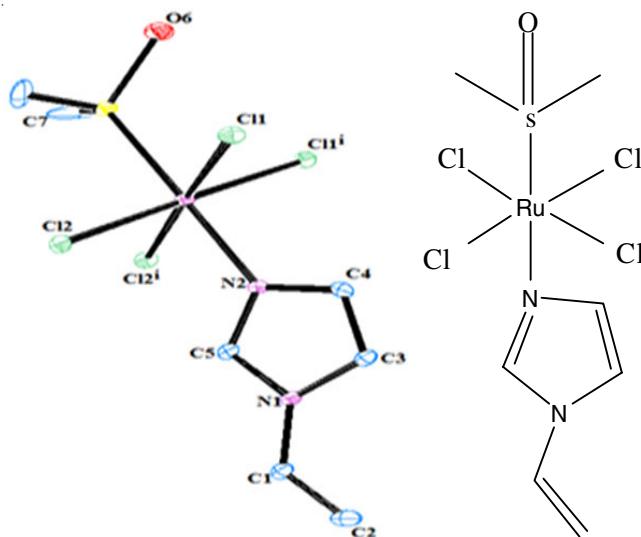


Fig. 6. Asymmetric unit of the crystal structure of Ru-VIMD complex

unit, Ru metal is coordinated to N-atom of vinylimidazole and 4-ethylaminomethyl pyridine ligand in both Ru-VIMD and Ru-EMP complex, dimethyl sulfoxide ligand coordinated through S-atom with Ru metal in both the structures. The Ru-VIMD complex crystallizes as orthorhombic system having a = 13.5309, b = 20.971, c = 7.0987 and α = 90°, β = 90°, γ = 90°. The crystal system of Ru-EMP complex is triclinic having a = 7.7110, b = 14.7774, c = 32.027(2) and α = 88.153, β =

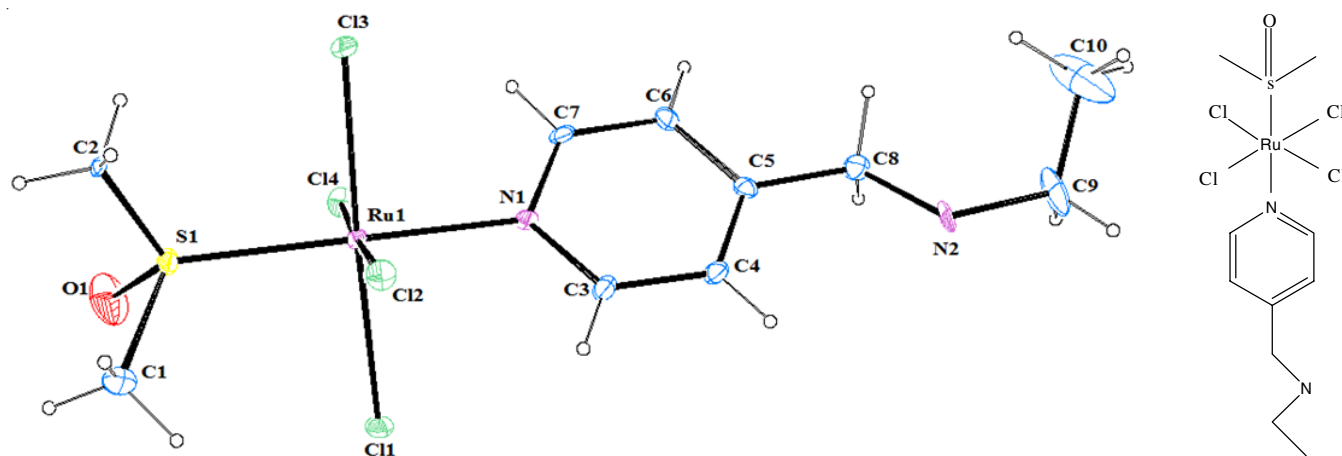


Fig. 7. Asymmetric unit of the crystal structure of Ru-EMP complex (eight asymmetric unit of Ru-EMP are found in the crystallographic structure)

83.225, $\gamma = 74.888$. The selected bond lengths and bond angles of Ru-VIMD and Ru-EMP complexes are given in Tables 2 and 3. The coordinated bond length, *i.e.* Ru-N bond length for Ru-VIMD complex is 2.180 Å and for Ru-EMP complex is 2.129 Å.

TABLE-2
SELECTED BOND DISTANCES (Å) AND
BOND ANGLES (°) Ru-VIMD COMPLEX

Bond length (Å)		Bond angle (°)	
Ru(1)-Cl(2)	2.334	N(8)-Ru(1)-Cl(3)	88.71
Ru(1)-Cl(3)	2.371	N(8)-Ru(1)-Cl(2)	89.68
Ru(1)-Cl(11)	2.280	S(4)-Ru(1)-Cl(2)	90.83
Ru(1)-Cl(12)	2.280	S(4)-Ru(1)-Cl(3)	90.79
Ru(1)-N(8)	2.180	Ru(1)-S(4)-C(14)	119.00
Ru(1)-S(4)	2.292	Ru(1)-S(4)-O(13)	113.78
C(9)-C(10)	1.344	O(13)-S(4)-C(14)	103.38
C(10)-N(8)	1.341	N(8)-C(5)-N(6)	110.88
C(11)-C(12)	1.343	N(6)-C(9)-C(10)	106.86
C(5)-N(6)	1.362	C(9)-C(10)-N(6)	109.45
C(5)-N(8)	1.312	C(5)-N(6)-C(11)	126.58

TABLE-3
SELECTED BOND DISTANCES (Å) AND
BOND ANGLES (°) Ru-EMP COMPLEX

Bond length (Å)		Bond angle (°)	
Ru(1)-Cl(3)	2.347	N(1)-Ru(1)-Cl(3)	88.01
Ru(1)-Cl(2)	2.336	N(1)-Ru(1)-Cl(2)	88.38
Ru(1)-Cl(13)	2.364	S(4)-Ru(1)-Cl(2)	92.75
Ru(1)-Cl(14)	2.345	S(4)-Ru(1)-Cl(3)	90.89
Ru(1)-N(5)	2.129	Ru(1)-S(4)-C(14)	93.81
Ru(1)-S(4)	2.292	Ru(1)-S(4)-O(13)	114.08
C(7)-C(6)	1.418	O(13)-S(4)-C(14)	105.07
C(7)-N(1)	1.390	N(1)-C(7)-C(6)	110.88
C(8)-C(5)	1.450	N(12)-C(9)-C(10)	111.33
C(8)-N(12)	1.526	C(9)-C(10)-N(12)	125.39
C(9)-N(12)	1.490	C(5)-N(12)-C(11)	119.63

Conclusion

Ruthenium complexes were synthesized with two biologically active ligands vinyl imidazole (VIMD) and 4-ethylaminomethyl pyridine (EMP). The synthesized complexes were found in crystalline form and found to be six coordinated. The DNA binding of these synthesized complexes were studied

by UV visible, fluorescence emission and electrochemical method. More hypochromism effect of Ru-EMP complex after adding CT-DNA has been observed. From cyclic voltammogram, it has been found after adding CT-DNA more current diminishes in Ru-EMP complex than Ru-VIMD complex. Emission intensity of Ru-EMP complex found to be higher than Ru-VIMD complex. The binding constant for Ru-VIMD and Ru-EMP complex were found to be 0.3181×10^5 and $0.936 \times 10^5 \text{ M}^{-1}$, respectively. The extent of spectral shift usually depends on the affinity of these complexes for interaction with CT-DNA. Synthesized complexes displayed moderate zone of inhibition against all the tested Gram-positive and Gram-negative bacterial strain. The positive shifts found for all the complexes indicate reliable binding of these complexes with CT-DNA. It was expected that the redox shifts obtained from electrochemical studies could also be contributed from the stacking interactions of substituted vinyl imidazole ligand within the base pairs of CT-DNA.

Supplementary file: The CCDC files No. 204955 and 2049756 contains the supplementary crystallographic data of the ruthenium(III) complexes of vinylimidazole (VIMD) and 4-ethylaminomethyl pyridine (EMP), respectively. These data can be obtained free of charge from the Cambridge Crystallographic Data Center *via* www.ccdc.cam.ac.uk.

ACKNOWLEDGEMENTS

The authors thank GUIST, Chemical Science for providing few instruments used to carry out this work.

CONFLICT OF INTEREST

The authors declare that there is no conflict of interests regarding the publication of this article.

REFERENCES

- I. Kostova, *Curr. Med. Chem.*, **13**, 1085 (2006); <https://doi.org/10.2174/092986706776360941>
- A.M. Bonin, J.A. Yanez, C. Fukuda, X.W. Teng, C.T. Dillon, T.W. Hambley, P.A. Lay and N.M. Davies, *Cancer Chemother. Pharmacol.*, **66**, 755 (2010); <https://doi.org/10.1007/s00280-009-1220-5>

3. B. Rosenberg, L. Van Camp and T. Krigas, *Nature*, **205**, 698 (1965); <https://doi.org/10.1038/205698a0>
4. M.J. Clarke, F. Zhu and D. Frasca, *Chem. Rev.*, **99**, 2511 (1999); <https://doi.org/10.1021/cr9804238>
5. A. Vessieres, W. Beck, E. Hillard and G. Jaouen, *Dalton Trans.*, 529 (2006); <https://doi.org/10.1039/B509984F>
6. C.M. Dupureur and J.K. Barton, *J. Inorg. Chem.*, **36**, 33 (1997); <https://doi.org/10.1021/ic960738a>
7. A. Mukherjee, R. Lavery, B. Bagchi and J.T. Hynes, *J. Am. Chem. Soc.*, **130**, 9747 (2008); <https://doi.org/10.1021/ja8001666>
8. M.J. Clarke, *Coord. Chem. Rev.*, **236**, 209 (2003); [https://doi.org/10.1016/S0010-8545\(02\)00312-0](https://doi.org/10.1016/S0010-8545(02)00312-0)
9. M.J. Clarke, *Met. Ions Biol. Syst.*, **42**, 425 (2004).
10. S. Leijen, S.A. Burgers, P. Baas, D. Pluim, M. Tibben, E. van Werkhoven, E. Alessio, E. Sava, G. Beijnen and J.H. Schellens, *Invest. New Drugs*, **33**, 201 (2015); <https://doi.org/10.1007/s10637-014-0179-1>
11. R.L.S.R. Santos, A. Bergamo, G. Sava and D. de Oliveira Silva, *Polyhedron*, **42**, 175 (2012); <https://doi.org/10.1016/j.poly.2012.05.012>
12. N. Mayorek, N. Naftali-Shani and N. Grunewald, *PLoS One*, **5**, e12715 (2010); <https://doi.org/10.1371/journal.pone.0012715>
13. M. Ogino, H. Hisatomi, M. Murata and M. Hanazono, *J. Cancer Res.*, **90**, 758 (1999).
14. Y. Eli, F. Przedeci, G. Levin, N. Kariv and A. Raz, *Biochem. Pharmacol.*, **61**, 565 (2001); [https://doi.org/10.1016/S0006-2952\(00\)00578-5](https://doi.org/10.1016/S0006-2952(00)00578-5)
15. C.T. Dillon, T.W. Hambley, B.J. Kennedy, P.A. Lay, Q. Zhou, N.M. Davies, J.R. Biffin and H.L. Regtop, *Chem. Res. Toxicol.*, **16**, 28 (2003); <https://doi.org/10.1021/tx020078o>
16. F. Dimiza, A.N. Papadopoulos, V. Tangoulis, V. Psycharis, C.P. Raptopoulou, D.P. Kessissoglou and G. Psomas, *Dalton Trans.*, **39**, 4517 (2010); <https://doi.org/10.1039/b927472c>
17. M. Benadiba, R.R.P. dos Santos, D.O. Silva and A. Colquhoun, *J. Inorg. Biochem.*, **104**, 928 (2010); <https://doi.org/10.1016/j.jinorgbio.2010.04.011>
18. G. Ribeiro, M. Benadiba, A. Colquhoun and D. de Oliveira Silva, *Polyhedron*, **27**, 1131 (2008); <https://doi.org/10.1016/j.poly.2007.12.011>
19. A.K.-W. Tse, H.-H. Cao, C.-Y. Cheng, H.-Y. Kwan, H. Yu, W.-F. Fong and Z.-L. Yu, *J. Invest. Dermatol.*, **134**, 1397 (2014); <https://doi.org/10.1038/jid.2013.471>
20. M.G. Chung, H.W. Kim, B.R. Kim, Y.B. Kim and Y.H. Rhee, *Int. J. Biol. Macromol.*, **50**, 310 (2012); <https://doi.org/10.1016/j.ijbiomac.2011.12.007>
21. L. Cheng, K.G. Abhilash and R. Breslow, *Proc. Natl. Acad. Sci. USA*, **109**, 12884 (2012); <https://doi.org/10.1073/pnas.1210846109>
22. G. Psomas and D.P. Kessissoglou, *Dalton Trans.*, **42**, 6252 (2013); <https://doi.org/10.1039/c3dt50268f>
23. G. Aridoss, S. Amirthaganesan, N. Ashok Kumar, J.T. Kim, K.T. Lim, S. Kabilan and Y.T. Jeong, *Bioorg. Med. Chem. Lett.*, **18**, 6542 (2008); <https://doi.org/10.1016/j.bmcl.2008.10.045>
24. C.G. Hartinger, M.A. Jakupec, S. Zorbas-Seifried, M. Groessler, A. Egger, W. Berger, H. Zorbas, P.J. Dyson and B.K. Keppler, *Chem. Biodivers.*, **5**, 2140 (2008); <https://doi.org/10.1002/cbdv.200890195>
25. S. Chennamaneni, B. Zhong, R. Lama and B. Su, *Eur. J. Med. Chem.*, **56**, 17 (2012); <https://doi.org/10.1016/j.ejmech.2012.08.005>
26. V. Feyer, O. Plekan, R. Richter, M. Coreno, M. de Simone, K.C. Prince, A.B. Trofimov, I.L. Zaytseva and J. Schirmer, *J. Phys. Chem.*, **114**, 10270 (2010); <https://doi.org/10.1021/jp105062c>
27. A.K. Chandra, D. Michalska, R. Wysokiński and T. Zeegers-Huyskens, *J. Phys. Chem. A*, **108**, 9593 (2004); <https://doi.org/10.1021/jp040206c>
28. S. Karabasannavar, P. Ailolli, I.N. Shaikh and B.M. Kalshetty, *Indian J. Pharm. Educ. Res.*, **51**, 490 (2017); <https://doi.org/10.5530/ijper.51.3.77>
29. M. Li, T. Lan, Z. Lin, C. Yi and G.-N. Chen, *J. Inorg. Chem.*, **18**, 993 (2013); <https://doi.org/10.1007/s00775-013-1048-7>
30. I. Ott, K. Schmidt, B. Kircher, P. Schumacher, T. Wiglenda and R. Gust, *J. Med. Chem.*, **48**, 622 (2005); <https://doi.org/10.1021/jm049326z>
31. F. Yuan, X. Chen, Y. Zhou, F. Yang, Q. Zhang and J. Liu, *J. Coord. Chem.*, **65**, 1246 (2012); <https://doi.org/10.1080/00958972.2012.670228>